

Non-equilibrium dynamics in amorphous $\text{Si}_3\text{B}_3\text{N}_7$

A. Hannemann, J.C. Schön, and M. Jansen

Max-Planck-Institut für Festkörperforschung, Heisenbergstr. 1, D-70569 Stuttgart, Germany

P. Sibani

Fysisk Institut, SDU, Campusvej 55, DK-5230 Odense, Denmark

We present numerical investigations of the dynamics on the energy landscape of a realistic model of the high-temperature ceramic $\text{a-Si}_3\text{B}_3\text{N}_7$. Below a critical temperature $T_c \approx 2000$ K the system is no longer in equilibrium, and we predict that the material has a glass transition in this temperature range at high pressure. Analyzing the two-time energy correlation function shows aging in this system, which is linked to the geometrical properties of the energy landscape.

PACS numbers: 02.50.r, 05.90.+m, 61.41.+e, 61.43.Fs, 64.70.Pf

Introduction: Amorphous nitridic ceramics containing both silicon and boron such as $\text{a-SiBN}_3\text{C}$ or $\text{a-Si}_3\text{B}_3\text{N}_7$ are synthesized via the sol-gel process[1] and are one of the most exciting new classes of high-temperature materials. Up to now, no crystalline form of these compounds is known. Under standard conditions $\text{a-SiBN}_3\text{C}$ is thermally stable and amorphous up to ≈ 2100 K, possesses excellent mechanical and elastic properties, e.g. a high bulk modulus of ca. 200 – 300 GPa, and is stable against oxidation in O_2 -atmosphere up to 1700 K[1]. These compounds appear to form covalent networks with a homogeneous distribution of the cations at least down to a scale of 1 nm[2] and pose many fascinating questions regarding their structure and physical properties.

Probing the glass transition of $\text{a-Si}_3\text{B}_3\text{N}_7$, the basic representative of nitridic ceramics, is experimentally difficult, since, under standard conditions, decomposition takes place at $T \approx 1900$ K, i.e. before the ceramic melts. This material is currently considered for high temperature engine applications and its aging properties are therefore of clear technological relevance, beside having theoretical interest within the general framework of glassy dynamics.

Determining whether a possibly non-ergodic system has "for all practical purposes" reached thermal (quasi-)equilibrium is not straightforward and possibly constitutes an ill-posed question. Physical properties of amorphous systems are known to drift with the time t_w , or age, elapsed since the quench into the glassy phase. For short observation times $t_{obs} \ll t_w$, the drift is undetectable and a state of quasi-equilibrium is revealed by the approximate validity of the fluctuation-dissipation theorem. Concomitant to the violations of the fluctuation-dissipation theorem for $t_{obs} > t_w$, the correlation and response functions acquire an additional dependence on t_w . This breaking of time translational invariance has been observed e.g. in the magnetic susceptibility of spin glasses, both in experiments[3] and model simulations[4, 5], in measurements of C_p for a-Se [6], and also in simulations of the dynamical structure factor of

e.g. a-SiO_2 above the glass transition temperature[7].

To detect ergodicity breaking we use 1) the specific heat C_V , which we calculate in three different ways, all agreeing in equilibrium but markedly differing if ergodicity is broken, and 2) the two-time energy-energy average $\phi(t_w, t_{obs}; T)$, and the related two-time autocorrelation function $C_E(t_w, t_{obs}; T)$. In quasi-equilibrium, the former equals one and the latter equals a generalized standard equilibrium specific heat $k_B T^2 C_V(t_w, t_{obs}; T)$. The age dependent C_V has been studied experimentally, e.g. for charge-density-wave systems[8], but does not appear to have been theoretically explored outside of two-level systems at very low temperatures[9].

Since aging is linked to the complexity of the energy landscape of the system, we have investigated some aspects of the latter, emphasizing their relation to the non-equilibrium dynamics.

Model and Techniques: The model of $\text{a-Si}_3\text{B}_3\text{N}_7$ consisted of 162 Si-atoms, 162 B-atoms and 378 N-atoms, respectively, in a $19.1 \times 19.1 \times 19.1 \text{ \AA}^3$ cubic box. As an interaction potential, we employed a two-body potential from the literature[10] based on *ab-initio* energy calculations of hypothetical ternary compounds which reproduces experimental data regarding the structure and vibrational properties of the binary compounds Si_3N_4 and BN and of molecules containing Si–N–B units.

The starting configurations for our simulations were generated by relaxation from high temperature melts [11]. The simulations were performed at fixed temperature and volume, with a Monte-Carlo algorithm using the Metropolis acceptance criterion. In each update, an atom is randomly selected for an attempted move in a random direction, and with an average size chosen to achieve an acceptance rate of ≈ 50 %. One Monte-Carlo cycle (MCC) corresponds to $N_{atom} = 702$ such individual moves. Note that the kinetic energy ($3/2kT$ per atom) does not appear in MC-simulations, and that all quantities studied relate to the configurational energy.

The temperatures investigated ranged from 25 to 7000 K. For each temperature up to 3000 K and above 3000

K, 9 and 3 runs, respectively, of length $t_{total} = 2 \times 10^5$ MCC were performed. In addition, for selected temperatures, ensembles of 100 runs of length $t_{total} = 10^6$ MCC were studied. The energy as function of time was registered every 10 MCC. Along the individual trajectories for $T = 250, \dots, 7000$ K, halting points x_H were chosen, from which both conjugate gradient minimizations ($x_H \rightarrow x_{min}^{(1)}$) and a set of 10 stochastic quenches ($T = 0$ K MC-runs) followed by conjugate gradient minimizations ($x_H \rightarrow x_Q \rightarrow x_{min}^{(2)}$) were performed. In the following, $t_{init} \approx 1000$ MCC is the initialization time of the MC-simulations needed for the system to reach equilibrium in the ergodic regime (i.e. at high temperatures), while $t_w \geq t_{init}$ is the waiting time before the observation begin.

Ergodicity : To investigate ergodicity versus temperature, we studied the specific heat C_V and the two-time energy-energy average

$$\phi(t_w, t_{obs}; T) = \frac{\langle E(t_w)E(t_w + t_{obs}) \rangle_{ens}(T)}{\langle E(t_w)E(t_w) \rangle_{ens}(T)}, \quad (1)$$

where the subscript "ens" always denotes an average over all trajectories. C_V was calculated using three different computational prescriptions. First

$$C_V^a(T) = \frac{\partial \langle \langle E \rangle_{t \in [t_w, t_{total}]} \rangle_{ens}(T)}{\partial T}, \quad (2)$$

where time averaging extends from t_w to the end of the simulation t_{total} and the temperature derivative is performed after the averaging. Secondly

$$C_V^b(T) = \frac{\langle E(T + \Delta T; t_w) \rangle_{t \in [t_w, t_w + t_{obs}]; t_{obs} \ll t_w}}{2\Delta T} - \frac{\langle E(T - \Delta T; t_w) \rangle_{t \in [t_w, t_w + t_{obs}]; t_{obs} \ll t_w}}{2\Delta T}. \quad (3)$$

This emulates a step experiment where the system ages at temperature T . The time averages over the observation time $t_{obs} \ll t_w$ are performed at temperatures $T \pm \Delta T$, where $\Delta T \approx 0.1T$. Finally we gauge the energy fluctuations in $[t_w, t_w + t_{obs}]$ by calculating

$$C_V^c(T) = \frac{\langle \langle E^2 \rangle_{t \in [t_w, t_w + t_{obs}]} - \langle E \rangle_{t \in [t_w, t_w + t_{obs}]}^2 \rangle_{ens}(T)}{k_B T^2}, \quad (4)$$

for a range of observation times t_{obs} which straddles t_w .

C_V^a has no t_{obs} dependence. By way of contrast, when increasing t_{obs} past t_w the observed dynamics in C_V^c changes from quasi-equilibrium to off-equilibrium (cf. inset in fig.1). C_V^b , which mimicks an experiment performed after some relatively long equilibration time t_w , likely yields the most "realistic" value for the specific heat for all temperatures. As shown in fig. 1 the above prescriptions yield, as expected, almost identical results in the high- T ergodic dynamical regime, but differ at low

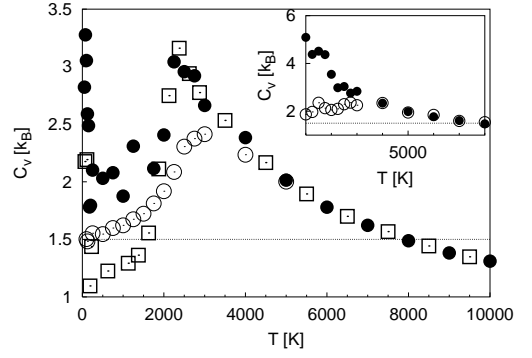


FIG. 1: Temperature dependence of the specific heats $C_V^{a,b,c}$. The waiting t_w and the observation times t_{obs} were 10^5 MCC for C_V^a (\square) and C_V^c (\bullet), and $t_w \geq 10^5$, $t_{obs} = 5 \cdot 10^3$ for C_V^b (\circ). Inset (note the different y-scale): C_V^c for $t_w = 10^4$, $t_{obs} = 10^4$ (\circ), 10^5 (\bullet). Note that $C_V^c \approx C_V^b$ for $t_{obs} \leq t_w$, while for $t_{obs} > t_w$ the two quantities differ.

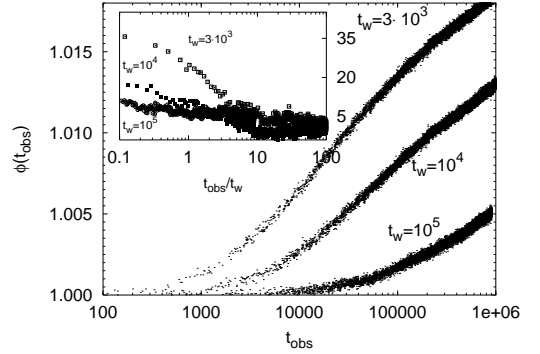


FIG. 2: Observation and waiting time dependences of the two-time energy-energy average $\phi(t_w, t_{obs}; T)$ for 1250 K, for an ensemble size of 100 runs (raw data). The inset shows the two-time autocorrelation function $C_E(t_w, t_{obs}; T = 1250K)$. Since, even for 100 runs (corresponding to ca. one year of CPU time on an AMD 1800+ MP processor), the scatter in C_E is relatively large, the data in the inset are averaged over ten time steps.

T . This indicates that below $T_c \approx 2000 - 3000$ K ergodicity is broken. Further evidence stems from the observation that for $T < T_c$, the motion is subdiffusive, while for $T > T_c$ standard diffusion is observed: For $T > T_c \approx 2100$ K, the diffusion coefficients for B, Si and N, follow a power law $D \propto (T - T_c)^\gamma$ with $\gamma = 1.7$, showing structural freezing-in. Similarly, the relaxation times associated with the bond survival probabilities of B-N and Si-N bonds display a rapid increase below T_c .

Repeating these investigations for a large number of volumes, we find a similar freezing-in of the structure for $T \approx T_c$. Furthermore, we determine a critical point in the liquid-gas region of the ternary system ($p_{cr} \approx 0.7$ GPa and, $T_{cr} \approx 3700K$). Since the tendency to decompose is greatly reduced for a supercritical fluid, we predict that a-Si₃B₃N₇ should exhibit a glass transition at a temperature $T_G \approx 1700 - 2000$ K and at a pressure of $p_G > 1$

GPa. Up to now, high-pressure experiments have only been performed for $T \approx 1000$ K and $p \approx 2.5$ GPa.

For $T > T_c$, the two-point correlation function always remains very close to the equilibrium value 1. The aging behavior in the glassy phase is shown in fig. 2 for $T = 1250$ K, and for three different waiting times $t_w = 3 \cdot 10^3, 10^4, 10^5$. In the non-equilibrium regime $t_{obs} \geq t_w$, ϕ is seen to deviate strongly from its equilibrium value $\phi_{eq} \equiv 1$. The closely related autocorrelation function $C_E(t_w, t_{obs}; T) \equiv \langle E(t_w) \cdot E(t_w + t_{obs}) \rangle_{ens} - \langle E(t_w) \rangle_{ens} \cdot \langle E(t_w + t_{obs}) \rangle_{ens}$ also exhibits the expected aging behavior, i.e. a marked decrease to zero from an almost constant value ($\propto C_V(t_w)$) once t_{obs} exceeds t_w . This monotonic dependence on t_w of the time range $t_{obs} \in [0, t_w]$ during which (quasi-)equilibrium behavior is still observed, correlates with the stiffening of the response of the system characteristic for aging processes: The longer the system is allowed to equilibrate, the longer is the subsequent time range during which equilibrium-like behavior is observed. This effect concurs with our observation that for $T \leq T_c$ we can fit $E(t; T)$ (and also $\langle E(t; T) \rangle_{ens}$) over the interval $[t_{init}, t_{total}]$ as a logarithmically decreasing function, $E(t; T) = E_0(T) - A(T) \ln\left(\frac{t}{t_0(T)}\right)$. Neglecting the fluctuations compared to the drift, one has $\phi(t_w, t_{obs}; T) \approx \frac{E(t_w + t_{obs})E(t_w)}{E(t_w)E(t_w)}$. Expanding ϕ for $t_{obs} \ll t_w$ then yields $\phi(t_w, t_{obs}; T) \approx 1 + \frac{A}{|E(t_w)|} \frac{t_{obs}}{t_w}$. Thus, $\phi(t_w, t_{obs}; T)$ substantially deviates from 1 for $t_{obs} > t_w$, as observed in the simulations. The inset shows $C_E(t_w, t_{obs}; T)$ plotted as function of the scaled variable t_{obs}/t_w . As t_{obs} increases, the data appears to collapse on a single curve, indicating that t_{obs}/t_w scaling can be expected to hold asymptotically.

Energy landscape: Finally, we would like to link the non-equilibrium behavior to the properties of the energy landscape of a-Si₃B₃N₇. Figure 3 shows the average energy $\langle E(t; T, x_{min}^{(1)}) \rangle_{ens}$ of local minima $x_{min}^{(1)}$ found by applying a conjugate gradient algorithm for logarithmically spaced halting points along several trajectories as a function of time for different temperatures.

We note that $\langle E(t; T, x_{min}^{(1)}) \rangle_{ens}$ decreases logarithmically with time for $T < T_c$ analogously to $\langle E(t; T) \rangle_{ens}$ [21]. A fit of the logarithmic slope yields $A(T) = 76.29 \cdot T - 134.56 \cdot T^2$, which qualitatively agrees with the low temperature expansion of $\langle E(t; T) \rangle_{ens}$ for the so-called LS-tree models[12], suggesting that the landscape of a-Si₃B₃N₇ might possess some hierarchical aspects in that energy range relevant for $T < T_c$.

For fixed simulation time, the deepest local minima are reached for $T = 1750$ K, which lies right below T_c . We find a similar behavior for the average energy $\langle E(T; x_{min}^{(2)}) \rangle$ of the local minima $x_{min}^{(2)}$ found after quenching plus gradient minimization starting from the holding points x_h , shown as a function of temperature in fig. 4. We clearly recognize a minimum in this curve at

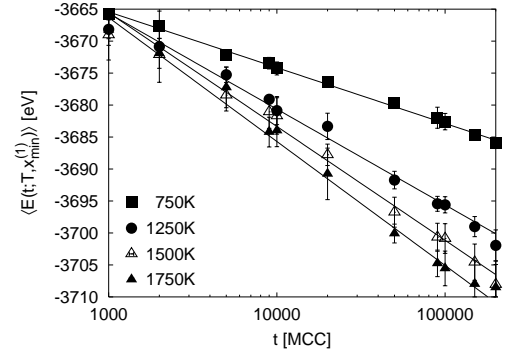


FIG. 3: Time dependence of the average energies $\langle E(t; T, x_{min}^{(1)}) \rangle_{ens}$ of the minima $x_{min}^{(1)}$ for selected temperatures $T = 750$ K, 1250 K, 1500 K, 1750 K.

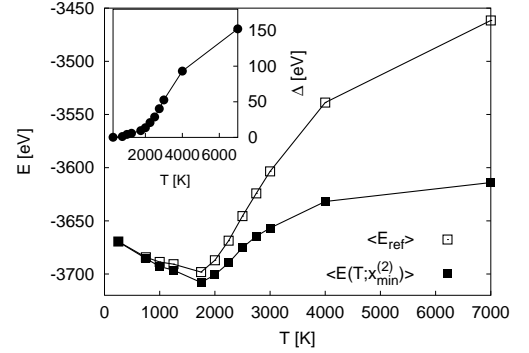


FIG. 4: Temperature dependence of the average energies $\langle \langle E(T; x_{min}^{(2)}) \rangle_{t_{obs}} \rangle_{ens}$ of the minima $x_{min}^{(2)}$ (Full squares). The open squares are values of reference energies $E_{ref}(T)$ (see text). The inset shows the temperature dependence of the excess energy Δ (see text).

$T \approx 1750$ K, and the largest increase occurs at $T \approx T_c$. Analogous observations are well-known from e.g. global optimization studies of complex systems, where it has been found that reaching the deepest local minima using Monte-Carlo-type search algorithms is achieved by spending most of the search time in the temperature interval slightly below the glass transition temperature[13]. Thus this result serves as another confirmation that ergodicity breaking is taking place at $T \approx T_c$.

The second curve in fig. 4 depicts $E_{ref}(T) = \langle \langle E(T, x_h) \rangle_{t_{obs}} \rangle_{ens} - (3/2)N_{atom}k_B T$. Note that if the motion around the minima were purely harmonic, $E_{ref}(T)$ would be the average energy of these minima. However, comparing $E_{ref}(T)$ with $\langle \langle E(T, x_{min}^{(2)}) \rangle_{t_{obs}} \rangle_{ens}$, we note that an excess energy $\Delta(T) = E_{ref}(T) - \langle \langle E(T, x_{min}^{(2)}) \rangle_{t_{obs}} \rangle_{ens} > 0$ exists. The growth of $\Delta(T)$ is monotonic in T and most pronounced for $T \approx T_c$. Clearly, in this temperature region the landscape below the halting points, which is "felt" by the walker, changes and a substantial shift to higher "reference" values for the vibrational contributions to the potential energy occurs.

Discussion: The computational analysis of a-Si₃B₃N₇

using $C_V^{a,b,c}$ and $\phi(t_w, t_{obs}; T)$ shows that this amorphous material can be expected to exhibit a glass transition with a concurrent break in the ergodicity at about $T_c \approx 2000$ K if pressures high enough to prevent decomposition are applied. Regarding its structural dynamics and aging properties for $T < T_c$, a-Si₃B₃N₇ exhibits a general behavior similar to standard test systems (Lennard-Jones, a-SiO₂) and CDW systems, insofar as we observe a freezing-in of the structure, and a waiting-time dependence of the two time correlation function and specific heat.

This aging phenomenon is related to the slow non-exponential relaxation dynamics on the energy landscape for $T < T_c$, resulting in a logarithmic drift towards lower energies. This applies both to the actual trajectories and the time-sequence of observed local minima. Independent of this aspect of the dynamics, we find that starting around T_c the average potential energy greatly exceeds the value associated with harmonic vibrations at T_c . 'Thermodynamically', this makes itself felt as a peak in the specific heat, which is often associated with the entropy due to an increased availability of additional amorphous configurations.

One possible origin for this excess energy is trapping [14, 15] due to an approximately exponential growth in the effective local density of states $g_{loc}(E) \propto \exp(\alpha(E - E_{min}))$, with the growth factor $\alpha = 1/T_{trap} \approx 1/T_c$. In such a case, the exponentially growing region of the deep pockets of the landscape becomes invisible for the random walker for $T > T_{trap}$, and the top of this region serves as the reference for the vibrational energy contribution. $\Delta(T)$ would thus refer to the depth of the exponentially growing pockets with $T_{trap} < T$. Studies of amorphous networks[16] and polymers[17] on lattices have suggested that such trapping might contribute to the glass transition in structural glasses.

Alternatively, the phase space volume of the locally ergodic regions around the saddle points might substantially exceed the one associated with local minima, such that these saddles serve as reference, as has been suggested for small Lennard-Jones systems[18]. Here, $\Delta(T)$ would correspond to the average energy difference between the relevant saddle points and the nearby local minima.

Landscape studies using the threshold algorithm[19], which can be used to estimate both local densities of states and minima, and the relative size of minimum and transition regions[20] could resolve this issue, but are not yet computationally feasible. Preliminary explorations of the region "below" the halting points by performing 10 quench runs for each halting point $x_h^{(i)}$ concur with the results obtained in[20] and show that a typical halting point is associated with only one rather circumscribed basin containing many similar minima, and not with a large region of the landscape encompassing very different structures. The latter would be expected if the dynamics

were dominated by high-lying saddle points.

Funding was kindly provided by the DFG via SFB408.

-
- [1] M. Jansen and P. Baldus, *Angewandte Chemie Int. Ed. Engl.* pp. 338–354 (1997).
 - [2] L. van Wüllen, U. Müller, and M. Jansen, *Angew. Chem. Int. Ed.* **39**(14), 2519 (2000).
 - [3] P. Nordblad and P. Svendlidh, *Spin Glasses and Random Fields* (World Scientific, Singapore, 1997), chap. 1, pp. 1–28.
 - [4] K. H. Hoffmann and P. Sibani, *Phys. Rev. A* **38**, 4261 (1988).
 - [5] J. P. Bouchaud, L. Cugliandolo, J. Kurchan, and M. Mezard, *Spin Glasses and Random Fields* (World Scientific, Singapore, 1997), chap. 7, pp. 161–224.
 - [6] R. Stephens, *J. Non-Cryst. Sol.* **20**, 75 (1976).
 - [7] W. Kob, *J. Phys.: Cond. Matter* **11**, R85 (1999).
 - [8] K. Biljakovic, J. Lasjaunias, P. Monceau, and F. Levy, *Phys. Rev. Lett.* **67**(14), 1902 (1991).
 - [9] D. Parshin and S. Sahling, *Phys. Rev. B* **47**(10), 5677 (1993).
 - [10] M. Gastreich, C. Marian, and J. Gale, *Phys. Rev. B* **62**, 3117 (2000).
 - [11] A. Hannemann, J. C. Schön, C. Oligschleger, and M. Jansen, in *Proceedings XX. DGK Workshop on amorphous solids*, edited by B. Müller, DGK (U. Jena, 1999), pp. 1–11, also cond-mat/000319.
 - [12] P. Sibani and K. H. Hoffmann, *Europhys. Lett.* **16**(5), 423 (1991).
 - [13] S. Kirkpatrick, C. D. Gelatt Jr., and M. P. Vecchi, *Science* **220**, 671 (1983).
 - [14] P. Sibani, J. C. Schön, P. Salamon, and J.-O. Andersson, *Europhys. Lett.* **22**, 479 (1993).
 - [15] J. C. Schön, *J. Phys. A: Math. Gen.* **30**, 2367 (1997).
 - [16] J. C. Schön and P. Sibani, *Europhys. Lett.* **49**, 196 (2000).
 - [17] J. C. Schön, *J. Phys. Chem. B* (2002), in press.
 - [18] A. Cavagna, *Europhys. Lett.* **53**, 490 (2001).
 - [19] J. C. Schön, *Ber. Bunsenges.* **100**, 1388 (1996).
 - [20] M. A. C. Wevers, J. C. Schön, and M. Jansen, *J. Phys. A: Math. Gen.* **34**, 4041 (2001).
 - [21] L. Angelani, R. Di Leonardo, G. Parisi, and G. Ruocco, *Phys. Rev. Lett.* **87**, 5502 (2001), find a similar behavior for 256 atom Lennard-Jones systems.